Development of highly sensitive TMR sensor

Mikihiko Oogane[1], Kosuke Fujiwara[2], Seiji Kumagai[2], Hitoshi Matsuzaki[2], and Yasuo Ando[1]
([1]Tohoku Univ., [2]Spin Sensing Corp.)

The magnetic tunnel junctions (MTJs)-based sensors (TMR sensor) are promising magnetic field sensor because of room temperature operation, small device size, and the low power consumption. Since the TMR sensors with such features are considered to be widely applicable not only to the magnetic recording, the TMR sensors will be a key device in the ICT and IoT societies. In addition, because of the dramatic increase in sensitivity of TMR sensors in recent years, the realization of the device that can detect the weak magnetic field of pico-Tesla such as bio-magnetic field is expected. We have already reported on the measurement of cardiac magnetic field (magnetocardiography: MCG) and brain magnetic field (magnetoencephalography: MEG) using TMR sensors [1], but, the further improvement in sensitivity and detectivity of TMR sensors is required to realize the actual TMR based-MCG and -MEG equipment. We will introduce recent progress in the development of highly sensitive TMR sensors.

We have achieved the lowest magnetic field detectivity of 1.0 pT / $Hz^{0.5}$ at 1 Hz in the TMR sensor using a magnetic flux concentrator (MFC) (Fig. 1). By using a TMR sensor with high magnetic field resolution in the low frequency region, we succeeded in measuring MCG at real-time and MEG with a small number of averaging times. Further, as shown in Fig. 1, the developed TMR sensor has an extremely low magnetic field detectivity of 0.1 pT / $Hz^{0.5}$ or less in the kHz band. Protons in the human body generate nuclear magnetic resonance (NMR) at a frequency of 1 to 3 kHz under a weak magnetic field of μT, and we succeeded in measuring the NMR signal for the first time using the TMR sensor (Fig. 2). These results show that the MEG signal and the magnetic resonance image (MRI) using NMR can be simultaneously measured by the same TMR sensor device.

This work was partly supported by JST S-innovation project, the Center for Innovative Integrated Electronic Systems (CIES), the Center for Science and Innovation in Spintronics (CSIS), and the Center for Spintronics Research Network (CSRN).

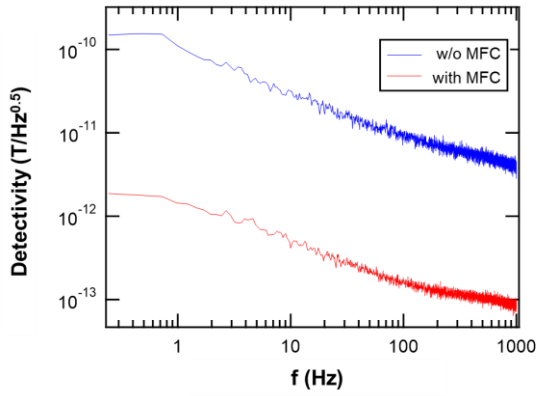

Fig. 1 Frequency dependence of detectivity in developed TMR sensors with/without magnetic flux concentrator (MFC)

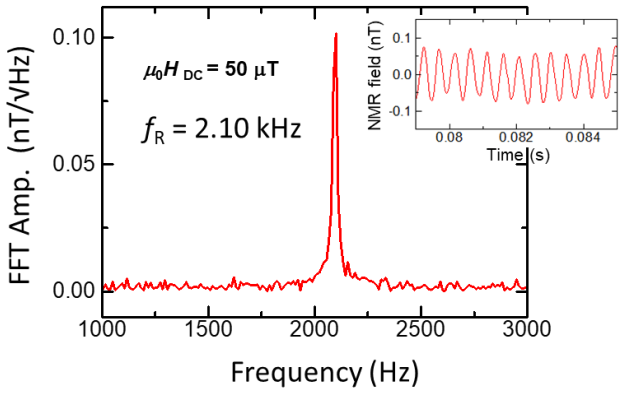

Fig. 2 Proton NMR signals under low magnetic field of 50 μT measured by developed TMR sensors with MFC.

Reference
1) K. Fujiwara *et al*., Appl. Phys. Express **11**, 023001 (2018).

偶関数型 GMR を用いた超高感度磁気センサ

東 祥弘，喜々津 哲，黒崎 義成，白鳥 聡志
(株式会社東芝　研究開発センター)
High sensitive magnetic sensor using symmetric response GMR
Yoshihiro HIGASHI, Akira KIKITSU, Yoshinari KUROSAKI and Satoshi SHIROTORI
Corporate Research and Development Center, Toshiba Corporation

偶関数特性を用いた変調システムによる超感度化のコンセプト

超高感度磁気センサは、2 次電池や半導体回路のリーク電流検査、鋼材の微細欠陥検査などの応用に期待されている(1)。中でも磁気抵抗効果 (MR) 素子 は高密度実装や集積化が容易なため、IoT などの幅広い用途が想定され、磁界検出感度は数 10 pT レベルが報告されている(2)。

MR 素子の高分解能実現のためには、素子の高出力化と低ノイズ化が求められる。前者は MR の増大や、測定磁場を集める MFC (Magnetic Flux Concentrator) の効率向上が検討されている(2)。後者は測定信号を高周波側にシフトさせる変調が注目されている(3)。MR 素子のノイズ成分としては半導体素子と同様に、周波数特性を持たないホワイトノイズ成分と周波数特性を持つ 1/f ノイズが発生する。今回は、MR 素子の磁場-抵抗 (R-H) 特性を利用して素子内で行う変調システムを検討した。

この変調システムは、(R-H) 特性が偶関数特性を示す巨大磁気抵抗 (GMR) 素子と、素子に近接して配置された銅配線で構成される (図 1 (a))。銅配線に、交流電流を印可することにより変流磁場H_{ac}が発生し、GMR 素子の R-H 特性により、測定磁場H_mが変調される (図 1 (b))。式(1)の磁場 H が偶関数特性の GMR 素子 (2 次関数に近似) に印可された場合の出力V_{out}は式 (2) で表すことができる。ここでH_mは、交流磁場周波数の側帯波$\omega_{ac} \pm \omega_m$ (第二項) に変調されることが分かる。また、図 1 (c) に示したように回路シミュレーションでも変調を確認した。

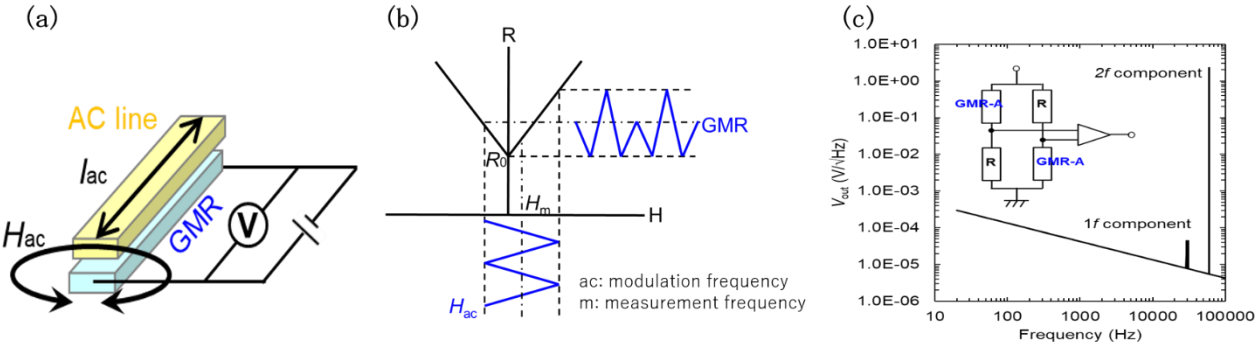

図 1. (a) 変調システムを有した磁気抵抗効果素子の模式図。(b) 交流磁場および測定磁場印可時の偶関数素子の R-H 特性。(c) 変調時のハーフブリッジ回路シミュレーション結果。

$$H = |H_m| * e^{-i\omega_m t} + |H_{ac}| * e^{-i\omega_{ac} t} \qquad (1)$$

$$V_{out} = \frac{dR}{dH}(H)^2 * I = \frac{dR}{dH}\left({H_m}^2 * e^{-2i\omega_m t} + 2|H_m| * |H_{ac}| * e^{-i(\omega_m - \omega_{ac})t} + {H_{ac}}^2 * e^{-2i\omega_{ac} t}\right)^2 * \mathrm{I} \qquad (2)$$

変調時の特有ノイズと考察

図2に実際に作成した素子周波数スペクトルを示す。変調しない場合、素子ノイズは測定周波数内で1/fノイズを示す (青線)。変調した場合、1 kHz以上の帯域においてフラットな周波数依存性をもつ特有ノイズ (ホワイトノイズ) が重畳された (赤線)。このホワイトノイズの発生のため、回路シミュレーションと比較して変調による低ノイズ化の効果が限定的となっている。本研究の目的はこれらのノイズのメカニズムを解明し、それを低減することで、これまでにない高感度磁気センサの実用化につなげることである。

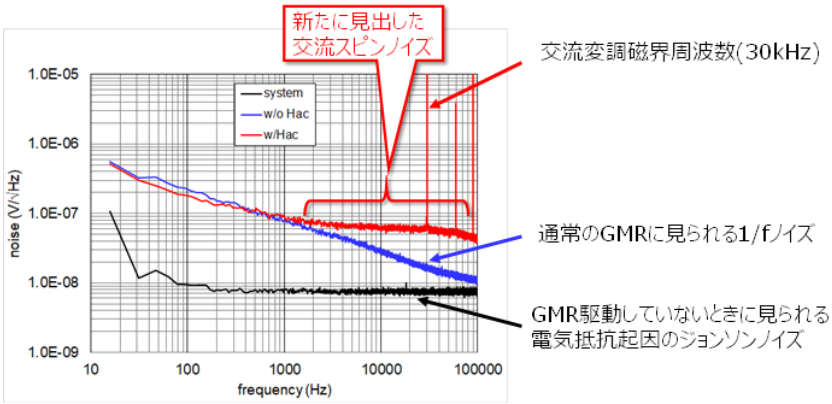

図 2. 作成した素子の高周波変調有無の周波数スペクトル。

図 3 (a) を用いてホワイトノイズが表れるメカニズムを考察する。低周波帯域 (領域 1) に 1/f ノイズを示すが、変調によって変調周波数 (1f) 近傍 (領域 3) に 1/f ノイズが重畳される。そのそれらの中間周波数帯域 (領域 2) では、元の 1/f ノイズと変調された 1/f ノイズの足し合わせにより、ホワイトノイズが発生したモデルを検討した。このモデルに基づいて、1/f ノイズが交流磁場周波数近傍に変調された場合の周波数スペクトルをベースに推定し、実験結果との比較を行った (図 3 (b))。実測されたノイズ (緑線) は、計算で求めたノイズ (赤線) よりも強度が大きく、かつスペクトル形状も異なっている。したがって、今回検討した 1/f ノイズの変調以外のメカニズムが示唆される。講演ではこれらの詳細を議論する。

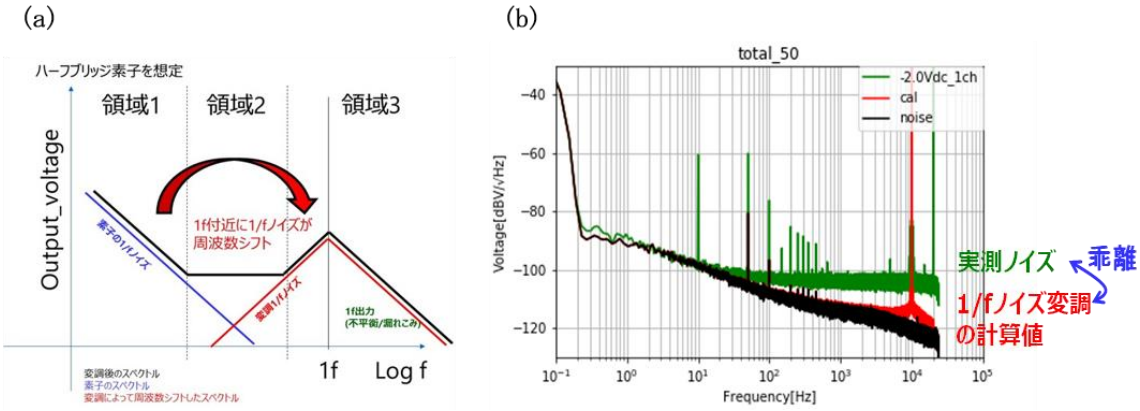

図 3.(a)変調時のホワイトノイズ発生モデル。(b)想定モデルの計算結果と実測ノイズ比較。

参考文献

(1) K. Kimura, Y. Mima, and N. Kimura, “Visualization of electric current density distribution—Application to nondestructive inspection for rechargeable batteries,” *J. Inst. Electr. Eng. Jpn*., vol. 135, no. 7, pp. 437–440, 2015.

(2) K. Fujiwara et al., “Magnetocardiography and magnetoencephalography measurements at room temperature using tunnel magneto-resistance sensors,” *Appl. Phys. Express*, vol. 11, no. 2, Feb. 2018, Art. no. 023001.

(3) W.Tian,et al., “Magnetic Flux Vertical Motion Modulation for 1/ **f** Noise Suppression in Magnetoresistance Field Sensors Using MEMS Device,”. *IEEE Trans. Magn.*, vol. 52, Issure:2, Feb. 2016, Art. no. 4000306.

This work was supported by the Cabinet Office (CAO), Cross-ministerial Strategic Innovation Promotion Program (SIP), “Intelligent Processing Infrastructure of Cyber and Physical Systems” (funding agency: NEDO)

New model of FM-OFG magnetometer with 1-pT noise floor

Ichiro Sasada
Sasada Magnetics and Sensors Laboratory

In this presentation, recent progress in the art of fundamental mode orthogonal fluxgate (FM-OFG) magnetometer and a new model of its embodiment will be presented.

The orthogonal fluxgate magnetometer was first reported by T. Palmer in 1953 [1], where a thin permalloy wire is used as a sensor core and ac excitation current is directly fed to the thin wire core. When magnetic field is input to the core, the induced voltage at the pickup coil that surrounding the core becomes to include second harmonics of the excitation frequency. When dc current is added as a bias to the ac excitation current to make them unipolar, the operation of the orthogonal fluxgate turns to the fundamental mode, which was introduced by I. Sasada 20 years ago [2]. The difference in the constituent is very little but the dc-bias current gives us a totally different picture in terms of noise [3]. Applications of very low noise FM-OFGs include MCG measurement [4], magnetic nano-particle detection [5] and small ferrous contaminants detection [6]. Recent developments include offset drift stabilization for long-term dc measurement [7] and noise reduction less than 1 pT/√Hz at 1 Hz [8]. The most important aspect of the FM-OFG is that it employs small angle rotation of magnetization in a thin magnetic wire or of a narrow magnetic ribbon. Therefore it can minimize any noises from Barkhousen jumps associated with domain wall motion. The operating principle is repeatedly explained in articles mentioned above. A key point is that the permeability along the core's length direction varies periodically with an excitation frequency. Fig. 1 shows a numerical result for this, where $H_{ex}=H_{dc}+H_{ac}$. Due to the periodical change in the permeability, low frequency magnetic field input produces amplitude modulation of the carrier frequency, which is exactly the excitation frequency. A block diagram of a magnetometer system with a negative feedback loop is shown in Fig. 2. This diagram is put in a box as shown in Fig. 3. Three output terminals are added to it; dc output (dc~1 kHz) with offset subtraction on demand via USB, two ac coupled outputs (0.16 Hz~1 kHz, 100 time gain and unity gain). A six volt ac adaptor supplies the power to it. Within the system, ±5 V is produced after filtering 6 V dc input. Power consumption of the main section is less than 0.2 W. Fig. 4 shows an example of one shot observation of a weak magnetic field coming out from a wrist watch's stepping motor using AC_100 output, in which several ringing peaks are visible due to 1 kHz frequency band and low system noise. A sensor head made of a 35 mm long thin core and a 30 mm long pickup coil is used. Measurement is carried out inside a shield. Fig. 5 shows a zoom-up of the first half segment of the trace in Fig. 4. The root-mean-square value of the zoomed up portion is calculated as 30.9 pTrms. By considering that the band width is 1 kHz, noise density per √Hz is 30.9/Sqrt[1000]=0.98 pT/√Hz. This is just a rough estimation of white noise. Another thing to be noted is that the peak-to-peak of white noise and the noise density per √Hz is very different in value when the observation frequency band is wide. Finally noise spectral densities are measured for two sensor heads; one is just mentioned and the other has a 30 mm long thin core. Sensor head under test is placed inside a five-shell cylindrical shield. Output voltages of the magnetometer are taken from the dc output

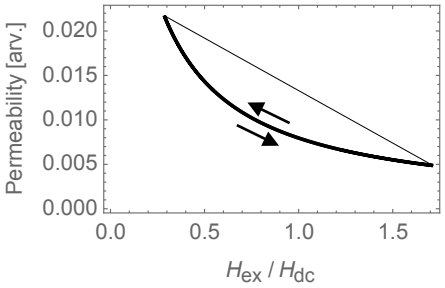

Fig. 1 Permeability along the length direction of a thin wire core is numerically calculated. Operating point traverses along the thick solid line periodically.

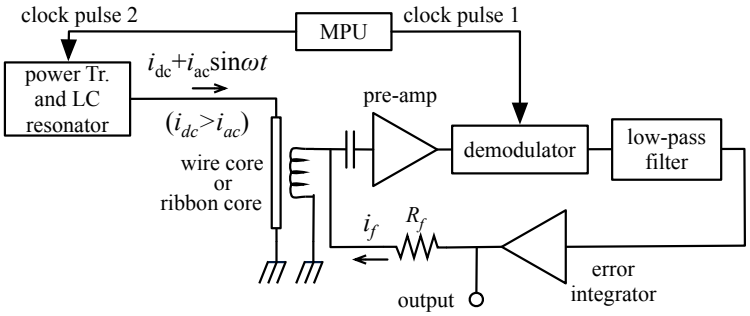

Fig. 2 Block diagram of FM-OFG magnetometer.

Fig. 3 New model of FM-OFG magnetometer.

inside the box then amplified 10 times by an external low noise amplifier with a 0.016 Hz cut-off high pass filter. Waveforms are recorded in 16 bits for 400 seconds with the sampling rate of 5 kS/s and band limited digitally to 2 kHz. FFT to calculate the noise spectral density is made in a PC. Results are shown in Fig. 6 for 35 mm long sensor head and in Fig. 7 for 30 mm long sensor head. In both plots, white noise region starts at around 10 Hz. The noise floor for the 30 mm long sensor head is 1.4 pT/√Hz and that for 35 mm one is 1.0 pT/√Hz. By elongating the thin core, one may get a higher sensitivity without excess increase in magnetic noise, hence one may get lower noise after scaling. With this scheme, 0.8 pT/√Hz@1Hz is realized in ref [8].

Reference

[1] T. M. Palmer, Proc. IEE Part II (London) 100, (1953) 545
[2] I. Sasada, Journal of Applied Physics, 91 (2002) 7789
[3] E. Paperno, Sensors and Actuators A 116 (2004) 405
[4] H. Karo et al., J. Appl. Phys. (2015); DOI: 10.1063/1.4918958
[5] H. Karo et al., AIP Advances 7, 056716 (2017); doi: 10.1063/1.4975655
[6] A. L. Elrefai et al., J. Appl. Phys. (2015); DOI: 10.1063/1.4913720
[7] N. Murata et al., IEEE Sensors Journal, DOI: 10.1109/JSEN.2018.2797961
[8] M. Janosek et al., IEEE Trans. Instrumentation and Measurement, 69, (2020) 2552

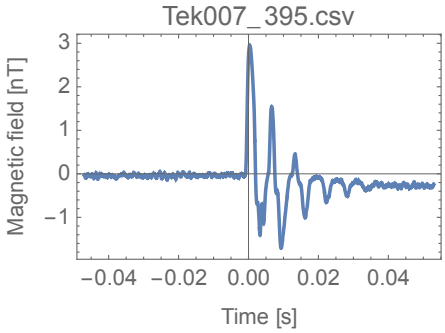

Fig. 4 Magnetic field from a stepping motor inside a wrist watch (Seiko Dolce). Distance from the bottom of the sensor core and the closer edge of the watch is about 11 cm.

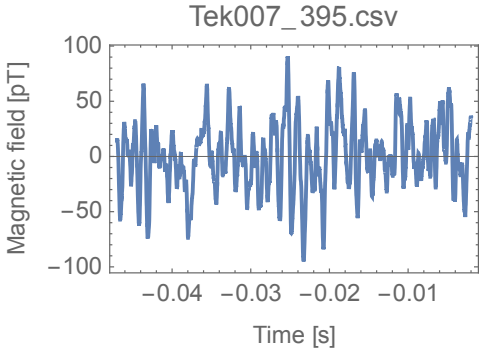

Fig. 5 Zoom-up of the left half part of the waveform in Fig. 4

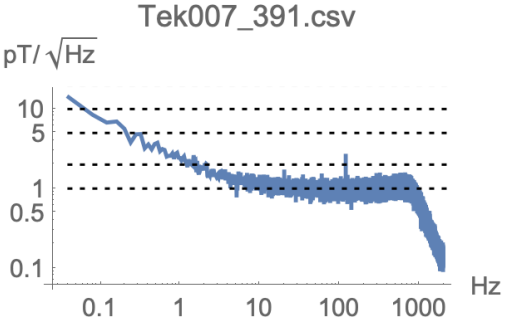

Fig. 6 Noise spectral density plot for a sensor head with 35 mm long core. Magnetometer used is FM-OFG sLab5 DC/AC1000.

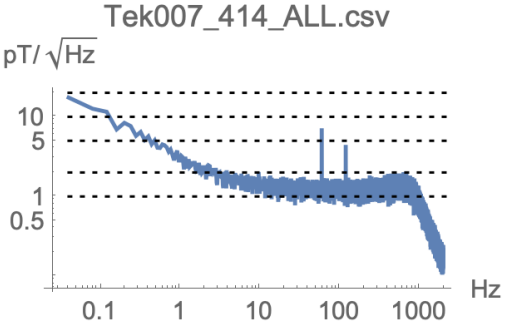

Fig. 7 Noise spectral density plot for a sensor head with 30 mm long core. Magnetometer used is FM-OFG sLab5 DC/AC1000.

Development of highly sensitive magnetoimpedance sensor system towards for sub-pico-tesla resolution

T. Uchiyama, J. Ma
Department of Electrical Engineering, Nagoya University, Nagoya 464 8603, Japan

The Magneto impedance (MI) sensor is a highly sensitive micro magnetic sensor based on the magneto-impedance effect in amorphous wires. As a high-performance magnetic sensor, magneto-impedance (MI) sensor has attracted considerable attention and has wide prospects in geomagnetic detection and bio-sensing. With the MI effect, when a high-frequency sine current is applied to a soft magnetic material, impedance of soft magnetic material changes significantly with external magnetic field. In MI sensor, the impedance change of Co-based amorphous wire increases with the frequency of excitation current. Meanwhile, in 1995, pulse driven MI sensor was developed with good linearity by using pick-up coil and higher change rate of impedance in amorphous wire which is more than 100%. In 2002, for distinguishing the poles of external magnetic fields, a pick-up coil was wound around the amorphous wire for detecting the induced voltage proportional to the impedance change (direction change of a magnetization vector) in pick-up coil.

Then, an electronic compass circuit using 3-axis amorphous wire CMOS MI sensor has been developed and mass produced for the mobile phone since 2005 by Aichi Steel Corporation, the smart phone since 2011, and the wristwatch since 2013 [1]. Meanwhile, Dr. L. G. C. Melo reported the theoretical limit of intrinsic magnetic field noise spectral density (MSD) of MI sensor [2], in 2008. The intrinsic magnetic field noise of 30-um Co-based amorphous wire is estimated to be about 10 fT measured over a bandwidth of 1Hz, with 1 cm length, in room temperature. However, with the conventional CMOS MI sensor circuit, it is difficult to examine the magnetic noise of the element in detail, such as comparing it with the theoretical, because of large 1/f noise of sensor circuitry.

In this study, we used 30 um diameter CoFeSiB amorphous wire samples in combination with the pick-up coil for magnetic field detector, which utilize off-diagonal MI effect [3]. The wire samples after heat treatment were supplied by Aichi Steel Corporation. In order to improve S/N ratio of the MI sensor system, we have developed new circuitry of pulse-driven MI sensor, which detecting both the positive peak and negative peak, which are excited by rising edge and drop edge of the excitation pulse. In this Pk-pk VD type MI sensor system [4], we have adopted the time-differential measurements between the voltages of the positive peak and negative peak. Because of the time-differential measurement of the same induced signal, that can reduce the common-mode noise due to the fluctuation of low frequency.

We have investigated the field detection characteristics (E_{out} versus H_{ex}) of the Pk-pk VD-type MI magnetometer by using different MI sensor heads with 400, 500, 600, 700, and 800 turns machinery pick up coils. These Pk-pk VD-type MI magnetometer have good linearity. We also investigated system sensitivities of the Pk-pk VD-type MI magnetometer and conventional MI magnetometer in case of the same amplifier gain (A = 10.8), at the end of circuits. The comparison of sensitivity depending on number of turns of pick-up coils between the Pk-pk VD-type MI magnetometer and conventional MI magnetometer is shown in Fig. 1. The highest sensitivity is 1.4×10^6 V/T at 500 turns. It is found that the sensitivity of the Pk-pk VD-type MI magnetometer is 1.3 times higher than the sensitivity of conventional MI magnetometer.

As shown in Fig. 2, we measured the output noises in time domain of the Pk-pk VD-type MI magnetometer and conventional MI magnetometer by using a low pass filter with a cutoff frequency of 10 Hz. The result illustrates the output noise of the Pk-pk VD-type MI magnetometer is reduced to less than 1/10 of conventional MI magnetometer. Obviously, we have markedly reduced the noise level in time domain of the Pk-pk VD-type MI magnetometer. The output RMS noise of Pk-pk VD-type MI magnetometer is approximately 5 pT with a 10 Hz low pass filter.

For further improving MI sensor, it’s necessary to analyzing intrinsic magnetic noise in amorphous wire. The noise of MI sensor is considered to be mainly due to circuit noise, fluctuation of wire magnetic moment (thermal magnetic noise), and irreversible movement of domain wall trapped by impurities and scratches on wire surface (Barkhausen noise). The noise level of Pk-pk VD Type MI sensor circuit is approximately 20 nV. The noise level we achieved here is getting close to the input conversion noise level of the differential amplifier used in this circuit. With this extremely low circuit noise we achieved here, we can investigate the intrinsic magnetic noise of amorphous wire via proposed MI

sensor circuit.

We have considered the loss due to the BH loop, and dealt with fluctuation of magnetic moment according to the general theory of fluctuation. When magnetic moment fluctuates due to thermal energy, it becomes noise of magnetic sensor measuring this magnetic moment. On the basis of this thermal fluctuation theory, the thermal noise of MI element can be expressed as a function of permeability, and it increases with anisotropy field. However, when anisotropy field is 3 Oe or more, the value tends to be saturated.

Moreover, the magnetization of amorphous wire is considered to be in circumferential direction, which is divided into several magnetic domains in opposite directions with 180◦ domain walls. Assuming the number of pinning sites such as scratches and impurities on the wire surface is constant, the greater the number of domain walls would lead to the greater the probability of being trapped at pinning sites. Noise analysis results suggests that the magnetic noise due to irreversible movement of domain wall increases with the number of domain walls.

Reference

1. K. Mohri *et al*., Journal of Sensors, (2015), Article ID 718069.
2. L. G. C. Melo *et al*., J. Appl. Phys., **103** (2008) 033903.
3. S. Sandacci *et al*., IEEE Trans. Magn. **40** (6) (2008) 18.
4. J. Ma *et al*., IEEE Trans. Magn. **53** (11) (2017) 4003404.

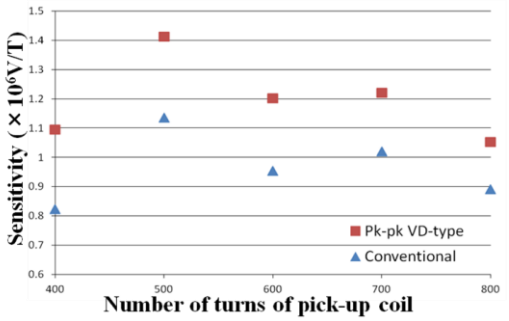

Fig.1 The comparison of sensitivity depending on number of turns of pick-up coil between the Pk-pk VD-type MI magnetometer and conventional MI magnetometer.

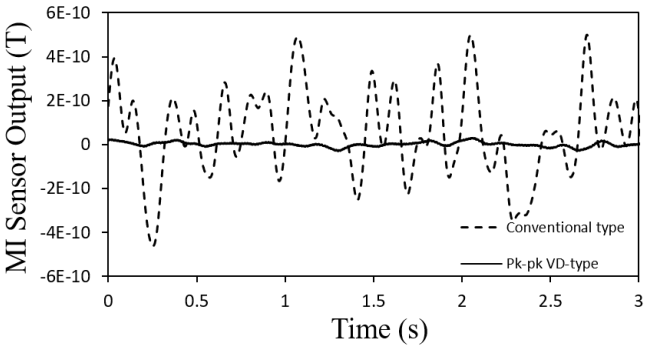

Fig.2 The output noises in time domain of the Pk-pk VD-type MI magnetometer and conventional MI magnetometer. The full curve shows output noises of the Pk-pk VD-type MI magnetometer. The dotted line shows output noises of conventional MI magnetometer. We used a low pass filter with a cutoff frequency of 10 Hz.

High-frequency drive type thin film sensor using coplanar line type structure and for biomedical application

S. Yabukami
Graduate School of Biomedical Engineering, Tohoku University, Sendai 980-8579, Japan

A very sensitive thin-film sensor was developed using a transmission line operating at room temperature. The sensor element consists of a coplanar line with amorphous-CoNbZr film. We already succeeded in the measurement of the MCG (magnetocardiogram) signals at 16 points without magnetic shielding, and these signals were found to roughly agree with MCG signals obtained with a SQUID (Superconducting Quantum Interference Device)[1]. However, the sensor system needs a magnetic coil (such as Helmholtz coil) to apply DC field, which results in increasing 1/f noise. In addition, this sensor is used with a high-frequency carrier of 1 GHz or higher, so we are considering the development and application of this sensor to ensure stable operation as a module mounted on a board without impairing the sensitivity of the sensor element. In the present study, we discuss direct bias to CoNbZr film and Cu film under a CoNbZr film and compare it with an application of bias magnetic field. We also have developed a straight coplanar line-type sensor with flip chip bonding. The high-frequency characteristics and sensitivity of the sensor element through comparison of cases with and without flip chip bonding was discussed. Good sensitivity with a phase change was obtained with flip chip bonding. Fig. 1 shows one example of a thin-film sensor. The sensor element consists of a meandering coplanar line, SrTiO film as an insulator, and an amorphous CoNbZr film and Cu film as an electrode. The coplanar structure was fabricated by the lift-off process. Amorphous CoNbZr film was deposited by RF sputtering on a glass substrate. In order to induce transverse magnetic anisotropy, a DC field of 0.3 T was applied during annealing after film deposition. Therefore, the easy axis, which was applied transverse to the coplanar line as shown in Fig. 1. SrTiO film was deposited by RF sputtering and annealed at 160°C during deposition. Cu and Cr film were deposited by RF sputtering. A high-frequency carrier flows in the center conductor of the coplanar line, not in the CoNbZr film, so the sensor is different from conventional GMI sensors in this respect. When this DC current flows directly in the CoNbZr film, permeability of the CoNbZr film changes, which results in the amplitude and the phase of the carrier is changed due to the skin effect and ferromagnetic resonance. Conventional wafer probes (GSG-40-150 and HFP-120-201) were put into contact with the sensor to apply carrier and DC current. The transmission coefficient (S_{21}) was measured by a network analyzer as the DC current was slowly changed. Fig. 2 shows the phase change (sensitivity) as a function of the DC field and carrier frequency. The sensor was connected with the flip chip bonding. The good phase change of about 290 degrees/Oe was obtained around 4 Oe and at 1.8 GHz. This proposed sensor can keep good sensitivity because the permeability was picked up in only the skin area of the magnetic thin film even if the dc field was not uniform inside the film.

Reference

1) S. Yabukami *et al*, *Journal of the Magnetics Society of Japan*, 38, 25(2014).

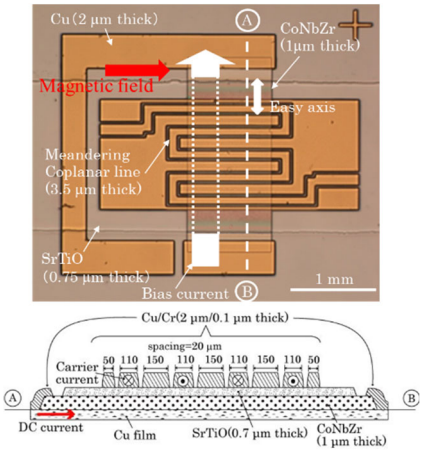

Fig. 1 Schematic view of the sensor.

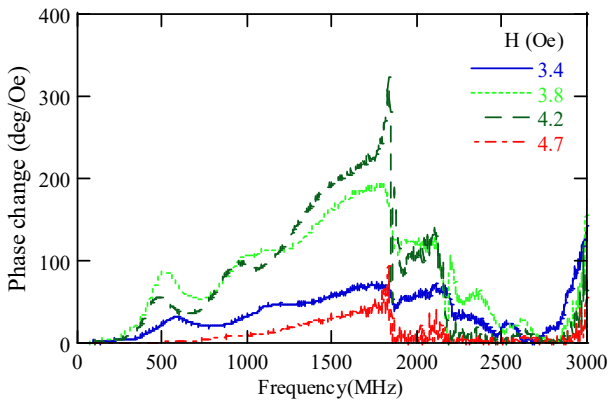

Fig. 2 Phase change of sensor output.

Diamond quantum sensor towards robust biosensing

Yuta Masuyama

(National Institutes for Quantum and Radiological Science and Technology)

Nitrogen-vacancy (NV) centers in diamond is a promising solid-state quantum sensor working at room temperature. The quantum sensor is a sensor that measures the physical quantity such as magnetic field by using the energy change of qubits [1]. By constructing an appropriate measurement system, the quantum sensor achieves high sensitive measurement with the quantum-limited noise. Thanks to the property of the diamond that is a wide bandgap semiconductor, the quantum coherence of the qubits maintains under a wide range of temperatures and pressures, including under room temperature and atmospheric pressure. This characteristic enables us to use the sensor for various applications including operating in vivo and extreme environments.

A highly sensitive sensor is used to detect small biological signals such as the magnetic field from the brain. However, the sensor detects noise sensitively as well as target signals. Thus, many kinds of highly sensitive sensors are limited to use in specific environments, e.g., magnetically shielded enclosures. The requirement of the magnetically shielded enclosure prevents the spread of technology due to its high cost and size. Noise can be environmental noise, control and measurement fluctuations in the sensor system, and noise from the sensor material. There are two ways to achieve robust biosensing against the noises. One is to reduce noise, and the other is to place the sensor as close as possible to the signal source.

We have developed a technology to reduce the environmental noise for the diamond quantum magnetometer with a large sensor volume by quantum operation using an enhanced microwave field [2]. The quantum operation work as a noise rejection filter for AC magnetic field sensing that enables us to achieve the magnetic field sensing with an AC magnetic field sensitivity of 3.6 pT /$\sqrt{Hz}$. For the sensing of DC magnetic signals, we have developed the gradiometer configuration [3]. Without any magnetically shielding, our gradiometer realizes a magnetic noise spectrum comparable to that of a three-layer magnetically shielded enclosure, reducing the noises at the low-frequency range below 1 Hz as well as at the frequency of 50 Hz (power line frequency) and its harmonics.

We are also improving the quality of the material for the diamond quantum magnetometer. The high-quality material improves the quantum coherence time of the NV center by reducing the spin noise from the material. Our institute has a technology of electron irradiation with high temperature and ion implantation. We constructed a fast evaluation system suitable for the material evaluation of the diamond quantum magnetometer, and are researching the relationship between NV center generation efficiency and coherence time by the electron beam irradiation.

Another method of noise reduction, i.e., bringing the sensor closer to the target, is quantum sensing using nanometer-scale diamonds. The NV center in a nanometer-scale diamond works as the quantum sensor, enabling us to inject the nanometer-scale diamond quantum sensor into a cell. The NV center can detect not only the magnetic field but also pH [4]. Thus, the nanometer-scale diamond quantum sensor gives us the local biological information.

Reference

1) C. L. Degen *et al.*, Rev. Mod. Phys. **89**, 035002 (2017)
2) Y. Masuyama *et al.*, Rev. Sci. Instrum. **89**, 125007 (2018)
3) Y. Masuyama *et al.*, Sensors **21**, 977 (2021)
4) T. Fujisaku *et al.*, ACS nano **13**, 11726 (2019)

Approaches to noise reduction of optically pumped magnetometers

Y. Ito and T. Kobayashi
(Kyoto University, Kyoto 615-8510, Japan)

Optically pumped magnetometers (OPMs) have extremely-high sensitivity comparable to the magnetometers with superconducting quantum interference devices (SQUIDs). The intrinsic sensitivity of the OPMs is limited by shot noise[1]:

$$\delta B \simeq \frac{1}{\gamma\sqrt{nT_2Vt}}, \tag{1}$$

where γ is gyromagentic ratio, n is atomic density, T_2 is relaxation time, V is sensing volume, and t is measurement time. δB is calculated as $\sim 10^{-17}$ T with the typical parameters in the spin-exchange relaxation-free (SERF) regime[2]. However, the sensitivity of practical OPMs has not reached such shot-noise limit yet. The OPMs in practical situation are affected by magnetic, optical, and electric noises, as shown in Fig. 1. The electric noise originating from electric circuits in the probe-beam detectors can be suppressed by low-noise and high-gain amplifiers. We fabricated the amplifier circuits for multi-channel OPMs, and obtained the coverted electric noise of 4.0 fT/Hz$^{1/2}$ in 10 channels[3].

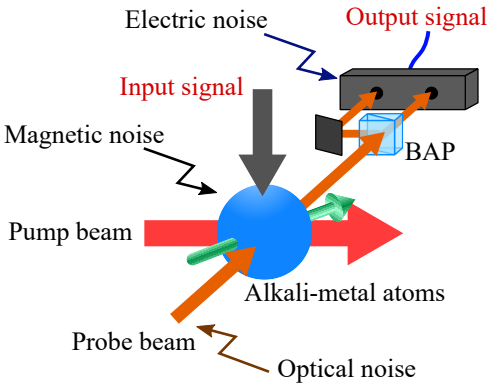

Fig. 1 Illustration of the pump-probe type OPM. BAP is a balanced amplified photodetector. The pump beam causes spin polarization of the alkali-metal atoms and the probe beam reads the fluctuation of the spin polarization caused by the input magnetic fields.

The optical noise is caused by convection effects in the probe beam path. To avoid such convection effects, enclosing the optics and the beam path is effective. In Fig. 1, we used a balanced amplified photodetector to detect the probe beam because it is convenient and free from extra electronics comparing to the detection method of the modulated probe beam and a lock-in amplifier, although the method using modulation can suppress the $1/f$ noise. In addition, we proposed hybrid cells enclosing two types of alkali-metal atoms such as K and Rb[4]. With the hybrid cell, the pumped atoms and the probed atoms are different, so that the probed atoms are immune to fluctuation caused by the pump beam[5]. Liu *et al.* reported that theoretical sensitivity of the OPM with a hybrid cell reaches 1.8×10^{-2} aT[6].

The magnetic noise is eliminated with high-performance magnetic shields and gradiometer configuration. The magnetic shields are extremely expensive, so that the gradiometer configuration is actively investigated. The best sensitivity of 0.16 fT/Hz$^{1/2}$ is also recorded by the gradiometer configuration[7]. We investigated two types of gradiometer configuration: optical gradiometer configuration[8] and differential measurement with balanced response[9]. These methods can effectively reduce the magnetic noise.

Recently, Limes *et al.* reported MCG and MEG operated with pulsed OPMs with gradiometer configuration under ambient environment[10]. They achieved 15.7 fT/cm/Hz$^{1/2}$ in Earth's ambient environment. These results suggested that the OPM research are moving to the next step.

References

1) D. Budker, W. Gawlik, D. F. Kimball, S. M. Rochester, V. V. Yashchuk and A. Weis: *Rev. Mod. Phys.*, **74**, 1153-1201 (2002).
2) J. C. Allred, R. N. Lyman, T. W. Kornack and M. V. Romalis: *Phys. Rev. Lett.*, **89**(13), 130801 (2002).
3) K. Nishi, Y. Ito and T. Kobayashi: *Opt. Express*, **26**(2), 1988-1996 (2018).
4) Y. Ito, H. Ohnishi, K. Kamada and T. Kobayashi: *IEEE Trans. Magn.*, **47**(10), 3550-3553 (2011).
5) M. V. Romalis: *Phys. Rev. Lett.*, **105**(24), 243001 (2010).
6) J.-H. Liu, D.-Y. Jing, L.-L. Wang, Y. Li, W. Quan, J.-C. Fang and W.-M. Liu: *Sci. Rep.*, **7**(1), 6776 (2017).
7) H. B. Dang, A. C. Maloof and M. V. Romalis: *Appl. Phys. Lett.*, **97**(15), 151110 (2010).
8) K. Kamada, Y. Ito, S. Ichihara, N. Mizutani and T. Kobayashi: *Opt. Express*, **23**(5), 6976-6987 (2015).
9) S. Ichihara, N. Mizutani, Y. Ito and T. Kobayashi: *IEEE Trans. Magn.*, **52**(8), 4002709 (2016).
10) M. Limes, E. Foley, T. Kornack, S. Caliga, S. McBride, A. Braun, W. Lee, V. Lucivero and M. Romalis: *Phys. Rev. Appl.*, **14**(1), 011002 (2020).